Single-parameter nonadiabatic quantized charge pumping

B. Kaestner*
Physikalisch-Technische Bundesanstalt, Bundesallee 100, 38116 Braunschweig, Germany

V. Kashcheyevs
Department of Physics, Ben Gurion University of the Negev, Beer Sheva 84105, Israel
and Institute for Solid State Physics, University of Latvia, Riga LV-1063, Latvia

S. Amakawa
Integrated Research Institute, Tokyo Institute of Technology, 4259-R2-17 Nagatsuta, Midori-ku, Yokohama 226-8503, Japan

M. D. Blumenthal
Cavendish Laboratory, University of Cambridge, Cambridge CB3 0HE, United Kingdom
and National Physical Laboratory, Hampton Road, Teddington TW11 0LW, United Kingdom

L. Li
Sichuan Normal University, No. 5, Jing'an Road, Chengdu, 610066 Sichuan, People's Republic of China

T. J. B. M. Janssen
National Physical Laboratory, Hampton Road, Teddington TW11 0LW, United Kingdom

G. Hein, K. Pierz, T. Weimann, U. Siegner, and H. W. Schumacher
Physikalisch-Technische Bundesanstalt, Bundesallee 100, 38116 Braunschweig, Germany
(Received 7 July 2007; published 14 April 2008)

Controlled charge pumping in an AlGaAs/GaAs gated nanowire by single-parameter modulation is experimentally and theoretically studied. Transfer of integral multiples of the elementary charge per modulation cycle is clearly demonstrated. A simple theoretical model shows that such a quantized current can be generated via loading and unloading of a dynamic quasibound state. It demonstrates that nonadiabatic blockade of unwanted tunnel events can obliterate the requirement of having at least two phase-shifted periodic signals to realize quantized pumping.

DOI: 10.1103/PhysRevB.77.153301 PACS number(s): 73.23.−b, 72.10.−d, 73.22.Dj

Single-electron pumps and turnstiles relating a dc current I to a driving frequency[1] f have attracted much interest, in particular, for their potential in metrological applications[2] and integrated single-electron circuits,[3] as well as for quantum information processing.[4] Most implementations exploit a very small isolated region coupled to leads through structures with tunable transparencies (e.g., tunnel barriers). The isolated region is so small that the addition or removal of even one electron makes an appreciable energetic difference. Modulation of the transparencies can lead to controlled entrance and exit of electrons to or from this region. Under appropriately chosen periodic modulation conditions, an integer number of electrons tunnel in and, subsequently, the same number of electrons tunnel out, resulting in a quantized current $I=nef$ ($n=1,2,3\ldots$; $-e$ as the electron charge). One way to achieve this is by the Coulomb blockade of tunneling using two or more single-electron transistors.[5–7] Another way is to directly tune the left and right tunnel barriers of a quantum dot (QD).[8–12]

In turnstile devices, a source-drain bias voltage is applied, which determines the direction of the quantized current. In contrast, charge pumps are operated at zero bias. Since in the adiabatic limit a single periodic perturbation cannot determine the direction of the current,[13] most models of quantized charge pumping[6,14–17] have assumed at least two parameters modulated out of phase. Also, electron pumps driven by only one gate[13,18–21] have been studied, but have not experimentally demonstrated the generation of quantized current.

In this Brief Report, we report the experimental demonstration of quantized charge pumping with single-gate modulation. Single-gate pumping is realized by using an unbiased QD and modulating only the entrance gate voltage. The analysis of a transparent quantum model confirms that quantized pumping is only obtained in the nonadiabatic regime and elaborates the conditions for the quantization.

In this Brief Report, measurements of two devices, A and B, will be discussed. The devices were realized by two 100-nm-wide metallic finger gates crossing a wire etched in an n-type AlGaAs heterostructure, as shown for a typical structure in Fig. 1. The distance between the gate centers was 250 nm. The lithographic width of the wire was about 500 nm in A and about 700 nm in B. All measurements were performed in a ^{3}He cryostat with a base temperature of 300 mK. For quantized charge pumping, the devices were operated in the following way: Both gates were tuned beyond pinch off by static voltages V_1 and V_2 applied to gates 1 and 2, respectively. A sinusoidal modulation of frequency f was coupled into gate 1 via a bias tee, as shown in Fig. 1. The power of the radio-frequency (rf) signal P^{rf} arriving at the gate was estimated to be about −23 dBm. By tuning V_2

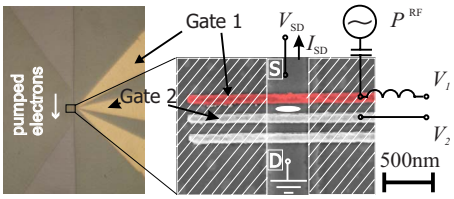

FIG. 1. (Color online) Picture of a typical device (left) with TiAu finger gates over the etched channel. In the scanning electron microscopy picture (right), bias and gate voltages are indicated, showing the gate colored in red as being modulated. The source (S) and drain (D) reservoirs are indicated. The hatched regions are depleted of the two-dimensional electron gas. A quasibound state is formed between gates 1 and 2, as indicated by the white ellipse. The direction of the pumped electrons is indicated by the white arrow on the left. The lowest gate is not in use in this experiment.

below a threshold value, electrons are pumped from source to drain, i.e., $I_{SD}<0$, as shown in Fig. 2(a). A finite bias voltage, $V_{SD}=+50\ \mu$V, was applied opposite to the pumping direction to prove the pumping regime. The results for different experimental conditions are offset in V_2 for clarity, plotting the current versus ΔV_2, which is the change in V_2. Four clear plateaus are observed in case (i) as ΔV_2 is varied from −5 to −50 mV. The ratio I_{SD}/ef *switches* between integer values to within the noise level of the measurement setup. We conclude that in this configuration, up to four electrons are robustly transferred in one cycle, depending on the value of V_2.

The tolerance in channel width was investigated by repeating the above measurements in device B having a lithographic channel width of about 700 nm. The corresponding pumped current is shown by the colored curves in Fig. 2(a). The transition regions between the plateaus are wider than in device A, but do not significantly change as the frequency is increased by almost an order of magnitude. The following examples are shown for frequencies in curves: (ii) 0.1 GHz, (iii) 0.47 GHz, and (iv) 0.8 GHz. The current values at fixed V_1 and V_2, corresponding to the first plateau, are plotted in Fig. 2(b) and show the expected linear dependence on f. Quantization was robust for the measured range of $P^{rf}=-26$ to −23 dBm, while the range of V_1 for which quantized pumping was observed increases with applied rf power P^{rf}.

For a quantitative theoretical analysis of the quantization mechanism, we consider a simple quantum model of noninteracting electrons confined in a one-dimensional wire and subjected to a time-dependent double-barrier potential, as plotted in the insets of Fig. 2,

$$U(x,t) = U_1(t)e^{-(x+x_0)^2/w^2} + U_2 e^{-(x-x_0)^2/w^2}, \qquad (1)$$

with a harmonically oscillating left barrier, $U_1(t)=U_1^{dc}-U_1^{ac}\cos(2\pi ft)$. The boundary conditions are defined by a Fermi distribution of electrons coming from the left, $f_F(\mu+eV_{SD})$, and from the right, $f_F(\mu)$, where μ is the electrochemical potential of electrons in the drain. Standard parabolic dispersion is taken for the wire assuming bulk GaAs effective electron mass of $m^*=0.067m_e$.

Full statistics of the stationary state in this model, including the dc current and the Fano factor, can, in principle, be obtained by solving the corresponding Floquet scattering problem.[13,22] However, the high number of excited side bands in the vicinity of the adiabatic limit renders such a calculation impractical. In order to proceed with the calculation, we restrict the parameters such that at all times there exists at least one quasibound state in the potential well formed between the barriers.

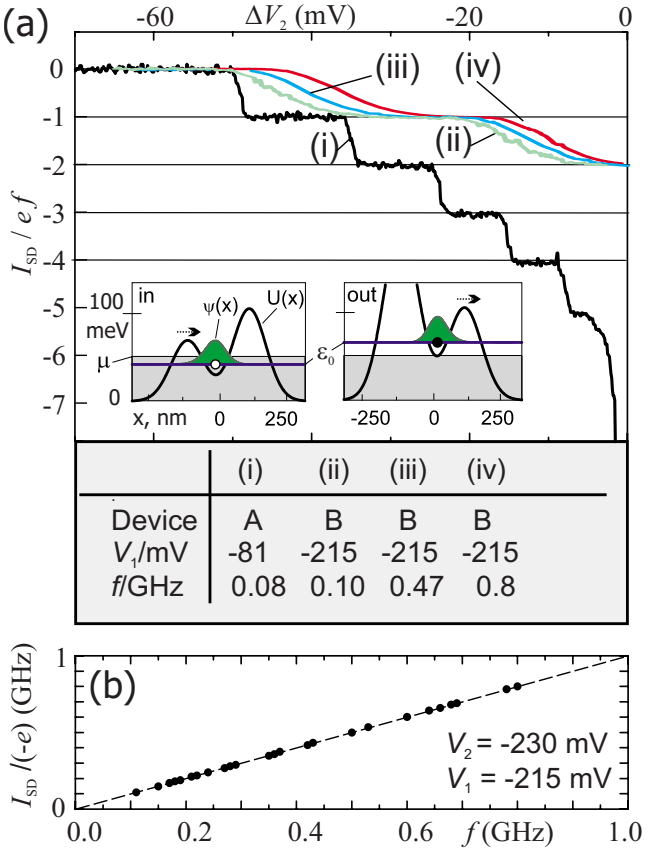

FIG. 2. (Color online) (a) Pumped current I_{SD} normalized by ef is shown versus the variation of the dc voltage applied to gate 2, ΔV_2. Experimental conditions are listed in the table. The corresponding results are offset in V_2 for clarity. Snapshots of the time-dependent potential U during loading and unloading of a single electron are shown in the insets. Calculated U and the wave function of the relevant transport state ψ correspond to the calculation presented in Fig. 3. (b) I_{SD} generated by device B when operated at different frequencies.

The instantaneous energy level $\epsilon_0(t)$ and its broadenings due to tunneling coupling to the left $\Gamma_L(t)$ and to the right $\Gamma_R(t)$ for the lowest of these states are obtained numerically by solving the frozen-time scattering problem and approximating the corresponding resonance with a Breit–Wigner formula.

The other quasibound states can be ignored if the gap from the lowest state, $\Delta\epsilon\equiv\epsilon_1-\epsilon_0$, is sufficiently large, such that $\Delta\epsilon>\mu-\epsilon_0$, hf, k_BT. It has been shown in Ref. 16 that exact results for *adiabatic* ($f\to 0$) pumping via a single resonance can be accurately approximated for $\Gamma\ll k_BT$ by solving a simple rate equation for the level occupation probability $P(t)$,

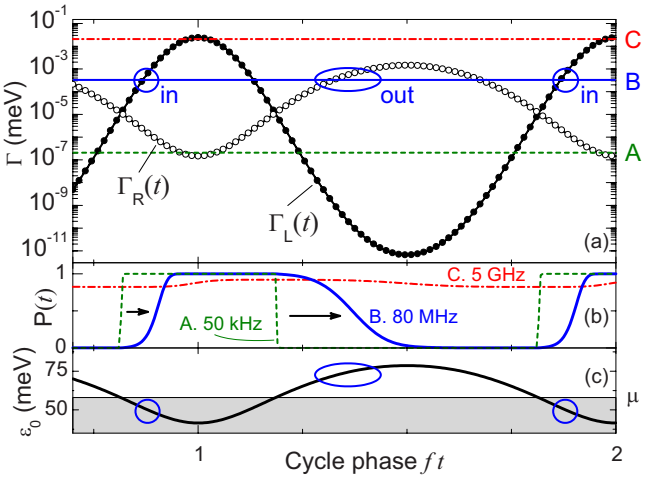

FIG. 3. (Color online) (a) Instantaneous values of the tunneling broadenings, $\Gamma_L(t)$ and $\Gamma_R(t)$, for the lowest quasilocalized energy level $\epsilon_0(t)$. The left barrier harmonically oscillates with an amplitude $U_1^{ac}=100$ meV around the value $U_1^{dc}=160$ meV; the right barrier is fixed at $U_2=120$ meV. Horizontal lines A, B, and C mark the energy quanta hf for the three representative frequencies, 50 kHz, 80 MHz, and 5 GHz, respectively. (b) Corresponding level occupation probability $P(t)$ at the selected frequencies. (c) Time evolution of the lowest quasilocalized energy $\epsilon_0(t)$. The blue ellipses indicate regions of charge transfer in regime B. Model parameters are $2x_0=250$ nm, $w=95$ nm, $\mu=58$ meV, and $T=300$ mK.

$$\hbar\dot{P} = (\Gamma_L + \Gamma_R)[f_F(\epsilon_0) - P] \tag{2}$$

(henceforth, we consider pure pumping only $V_{SD}=0$).

We shall assume Eq. (2) to hold also in the nonadiabatic regime as long as the only characteristic energy scales allowed to be less than hf are the tunneling widths Γ_L and Γ_R.[27] The average dc current, $I=eNf$ (where N is a real number), is then easily calculated by separating the left and right contributions to the full tunneling current on the right-hand side of Eq. (2). Physically, this assumption corresponds to neglecting the dynamics of hot electrons and holes outside the double-barrier structure.

Results of our calculations, summarized in Figs. 3 and 4, reveal three physically different transport regimes: (A) small next-order nonadiabatic corrections,[23] $N \propto f$, to the symmetry-dictated[13] adiabatic limit $N(f \to 0)=0$; (B) current quantization, $N \approx 1$, as achieved in the present experiment; and (C) crossover to approximately frequency-independent current, $N \propto f^{-1}$. Typical evolution of the tunnel couplings during one cycle is shown in Fig. 3(a). Γ_L changes exponentially because of the modulation of the left barrier height U_1, while Γ_R changes mainly due to oscillations in ϵ_0. Quantities $\log \Gamma_L(t)$, $\log \Gamma_R(t)$, and $\epsilon_0(t)$ can be well approximated by a few Fourier harmonics.

The qualitative behavior of our pumping model is determined by the extent of nonadiabaticity. At finite frequency f, the transport becomes blocked as soon as the corresponding tunneling coupling Γ becomes less than a characteristic scale of order hf.[13,24] Three representative values of hf are indicated in Fig. 3(a) corresponding to the scenarios A, B, and C.

In the weakly nonadiabatic regime (A), the QD and at least one of the two reservoirs remain nearly in their instantaneous equilibrium, and the occupation probability is close to $P(t) \approx f_F[\epsilon_0(t)]$ [see curve A of Fig. 3(b)]. Transitions of $P(t)$ between 0 and 1 (charge loading and unloading of Ref. 16) in this case appear as sharp steps at the instants the transport level crosses the Fermi level, $\epsilon_0(t)=\mu$, which can be obtained from Fig. 3(c). Because of the presence of only one pumping parameter, the ratio Γ_L/Γ_R has a strictly zero (mod π) phase shift to $\epsilon_0(t)$. Therefore, Γ_L/Γ_R is the same at these two charge transfer points, and the net pumped charge vanishes in the adiabatic limit.[13,25]

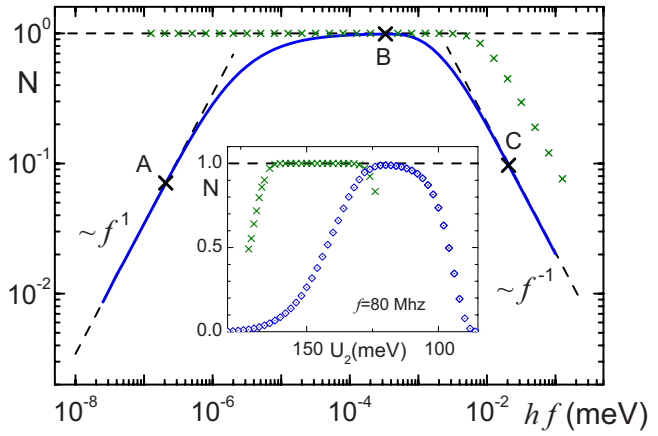

FIG. 4. (Color online) Calculated average number of pumped electrons per cycle as a function of driving frequency. Model parameters of the blue continuous curve are the same as in Fig. 3. Green crosses show the result with a different optimized set of parameters giving a wider frequency range for quantized charge pumping. Inset: blue symbols show the number of pumped electrons at the experimental frequency $f=80$ MHz (point B on the continuous line in the main plot) as a function of the barrier height U_2 and otherwise identical parameters as in Fig. 3. Green crosses indicate the result with the optimized set of parameters as above.

A qualitative difference from the nearly adiabatic regime (A) is observed once the frequency is high enough (B). Then, loading ("in") and unloading ("out") are delayed with respect to crossing of the Fermi level. The reason for the delay is that both tunnel rates, $\Gamma/\hbar$, are much smaller than the driving frequency f when crossing the Fermi level. Thus, tunneling is too slow to induce the charge transfer, which we refer to as nonadiabatic blockade of tunneling. It is only when Γ_L (Γ_R) grows sufficiently large for loading (unloading) that tunneling becomes effective and $P(t)$ switches from 0 to 1 (from 1 to 0), resulting in integer charge transfer from left to right in one cycle (see regions marked by ellipses in Fig. 3 and corresponding potential snapshots in Fig. 2). Note that the reverse process (tunneling back in the wrong direction) after subsequent crossing of the Fermi level is suppressed because of nonadiabatic blockade of tunneling.

Frequency increase beyond the optimal range of operation would lead to incomplete loading and unloading, and as a result, reduce the accuracy. This reduction is similar to the degrading role of nonadiabaticity discussed in Ref. 24. Eventually, in the high-frequency regime (C), of our model, the tunneling events become rare on the time scale of a single period, and the occupation probability $P(t)$ approaches a

constant time-averaged value, $\overline{(\Gamma_L+\Gamma_R)f_F(\epsilon_0)}/\overline{(\Gamma_L+\Gamma_R)}$.

The results of the calculation of the average charge transfer per cycle are shown in Fig. 4 (continuous line) for a range of frequencies using the same parameters as in Fig. 3. Changing the potential on gate 2 reveals the current quantization step shown by the blue diamonds in the inset of Fig. 4. The overlap of regime (B) with regime (A) or (C) results in a deviation of the number of charges transferred per cycle from 1 and constitutes a main source of error. It depends crucially on the barrier shape. By introducing an extra parameter in Eq. (1) which controls the degree of screening of the potential inside the leads, the frequency range of regime (B) can be extended, as shown by the green crosses in Fig. 4. Also, the quantization plateau in the inset is significantly wider. An accuracy of <10 ppb (ppb denotes parts per 10^9) has been numerically obtained. An unwanted surplus of electrons in the QD (involvement of more than two charge states) might be another source of error which is not accounted for in our model calculation. It occurs roughly with a probability of about e^{-E_C/k_BT}, where E_C is the charging energy of the dot. However, with $E_C \approx 1$ meV (determined for device B in the open regime) and $T=300$ mK, this mechanism is negligible compared to the error discussed above.

In conclusion, we have demonstrated quantized charge pumping under unconventional conditions, namely, modulating only a single parameter and in the nonadiabatic regime. The principle of operation is analyzed by using a simple quantum mechanical model, showing the essential role of nonadiabaticity for the pump to work. A key advantage over multiple-parameter pumps is that the operation of many pumps in parallel is greatly simplified and hence the realization of a substantial increase in quantized current output should be possible as needed for fundamental experiments in metrology.

Note added. During the review process of our Brief Report, experimental studies have been reported by Fujiwara *et al.*,[26] which demonstrate quantized single-gate pumping. The material system in those works is different from the one in our study. These results testify to the broad portability of the nonadiabatic single-gate pumping mechanism.

The authors acknowledge fruitful discussions with T. Altebaeumer, S. Kohler, H. Scherer, and F. J. Kaiser. V.K. acknowledges financial support from German-Israeli Project Cooperation (DIP), Israel Science Foundation, and Latvian Council of Science.

*bernd.kaestner@ptb.de

[1] D. V. Averin and K. K. Likharev, *Mesoscopic Phenomena in Solids* (Elsevier, Amsterdam, 1991), pp. 173–271.
[2] I. M. Mills, P. J. Mohr, T. J. Quinn, B. N. Taylor, and E. R. Williams, Metrologia **43**, 227 (2006).
[3] K. Nishiguchi, A. Fujiwara, Y. Ono, H. Inokawa, and Y. Takahashi, Appl. Phys. Lett. **88**, 183101 (2006).
[4] C. H. W. Barnes, J. M. Shilton, and A. M. Robinson, Phys. Rev. B **62**, 8410 (2000).
[5] L. J. Geerligs, V. F. Anderegg, P. A. M. Holweg, J. E. Mooij, H. Pothier, D. Esteve, C. Urbina, and M. H. Devoret, Phys. Rev. Lett. **64**, 2691 (1990).
[6] H. Pothier, P. Lafarge, C. Urbina, D. Esteve, and M. H. Devoret, Europhys. Lett. **17**, 249 (1992).
[7] M. W. Keller, J. M. Martinis, N. M. Zimmerman, and A. H. Steinbach, Appl. Phys. Lett. **69**, 1804 (1996).
[8] L. P. Kouwenhoven, A. T. Johnson, N. C. van der Vaart, C. J. P. M. Harmans, and C. T. Foxon, Phys. Rev. Lett. **67**, 1626 (1991).
[9] M. Switkes, C. M. Marcus, K. Campman, and A. C. Gossard, Science **283**, 1905 (1999).
[10] A. Fujiwara, N. M. Zimmerman, Y. Ono, and Y. Takahashi, Appl. Phys. Lett. **84**, 1323 (2004).
[11] J. Ebbecke, N. E. Fletcher, T. J. B. M. Janssen, F. Ahlers, M. Pepper, H. E. Beere, and D. A. Ritchie, Appl. Phys. Lett. **84**, 4319 (2004).
[12] M. D. Blumenthal, B. Kaestner, L. Li, S. Giblin, T. J. B. M. Janssen, M. Pepper, D. Anderson, G. Jones, and D. A. Ritchie, Nat. Phys. **3**, 343 (2007).
[13] M. Moskalets and M. Büttiker, Phys. Rev. B **66**, 205320 (2002).
[14] D. J. Thouless, Phys. Rev. B **27**, 6083 (1983).
[15] Y. Levinson, O. Entin-Wohlman, and P. Wölfle, Physica A **302**, 335 (2001).
[16] V. Kashcheyevs, A. Aharony, and O. Entin-Wohlman, Phys. Rev. B **69**, 195301 (2004); arXiv:cond-mat/0308382v1.
[17] P. A. Maksym, Phys. Rev. B **61**, 4727 (2000).
[18] L. P. Kouwenhoven, A. T. Johnson, N. C. van der Vaart, A. van der Enden, C. J. P. M. Harmans, and C. T. Foxon, Z. Phys. B: Condens. Matter **85**, 381 (1991).
[19] T. Altebaeumer, S. Amakawa, and H. Ahmed, Appl. Phys. Lett. **79**, 533 (2001).
[20] L. Arrachea, Phys. Rev. B **72**, 125349 (2005).
[21] L. E. F. Foa Torres, Phys. Rev. B **72**, 245339 (2005).
[22] S. Kohler, J. Lehmann, and P. Hänggi, Phys. Rep. **406**, 379 (2005).
[23] O. Entin-Wohlman, A. Aharony, and Y. Levinson, Phys. Rev. B **65**, 195411 (2002).
[24] K. Flensberg, Q. Niu, and M. Pustilnik, Phys. Rev. B **60**, R16291 (1999).
[25] P. W. Brouwer, Phys. Rev. B **58**, R10135 (1998).
[26] A. Fujiwara, K. Nishiguchi, and Y. Ono, Appl. Phys. Lett. **92**, 042102 (2008).
[27] In the limit $\max(\Gamma, hf) \ll k_BT$, our Markovian rate equation [Eq. (2)] can be explicitly derived from the exact time evolution equation for the occupation number of a single weakly coupled level [Eq. [10] of Ref. 24].